Available online at www.sciencedirect.com
ScienceDirect
Journal of Photochemistry and Photobiology A: Chemistry 192 (2007) 159–165
Journal of Photochemistry and Photobiology A:Chemistry
www.elsevier.com/locate/jphotochem

The synthesis and optical properties of GaSe/InSe core/shell nanoparticles

Shuming Yang [a,*], Hongjun Wang [a], Wenhong Fu [a], David F. Kelley [b]

[a] *College of Chemistry and Chemical Engineering, Xinyang Normal University, Henan 464000, China*
[b] *School of Natural Sciences, University of California, Merced, Merced CA 95344, USA*

Received 12 February 2007; received in revised form 12 April 2007; accepted 16 May 2007
Available online 18 May 2007

Abstract

The synthesis of epitaxially grown GaSe/InSe core/shell nanoparticles is reported. InSe shells of 0.25 nm in thickness are grown on GaSe cores of 6 nm in diameter. The shell growth is accompanied by a red shift of the absorption spectrum and a decrease of the room temperature emission intensity. The absorption onset on red side just remains unchanged but that on blue side shifts from 27,840 to 25,266 cm^{-1}, which means that an electron transition occurs between the GaSe core and the InSe shell. Time resolved emission experiments are also performed on the GaSe and the GaSe/InSe core/shell nanoparticles. Emission decay takes place on the 80 ps, 400 ps, and 2.4 ns time scales, while anisotropy decay follows two stages of 400 ps and 2.4 ns. Relaxation kinetics shows that the deep hole traps are effectively suppressed in the GaSe/InSe core/shell nanoparticles. The electron transition between the GaSe core and InSe shell results in a degree of charge separation that makes this core/shell nanoparticle attractive for use in photoelectric conversion devices.

Keywords: GaSe/InSe core/shell nanoparticle; Absorption transition; Anisotropy; Time resolved emission

1. Introduction

There has been a growing interest in the spectroscopic and photophysical properties of semiconductor nanoparticles, also referred to as quantum dots. Despite this interest, relatively few types of semiconductor nanoparticles have electronic, optical, and photophysical properties that are well understood. This is particularly true for III–VI layered semiconductors. The III–VI compounds, such as InSe and GaSe, are layered semiconductors in which a primitive layer consists of four atomic planes, Se–M–M–Se (M = In, Ga). The selenium atoms form two-dimensional hexagonally close-packed sheets, giving these crystals their hexagonal structure. The metal atoms are aligned along the *c* axis in every other trigonal prismatic site [1]. The band gaps of III–VI layered semiconductors are generally narrow at room temperature, which makes it an attractive material for solar energy conversion and optoelectronic devices [2,3]. Due to the absence of dangling bonds on the (0 0 1) surface, it has the potential to be used for heterojunction device applications with a low density of interface states [4,5].

We have recently reported much of the spectroscopy and photophysics of GaSe nanoparticles [6–10] and strongly interacting aggregates of these particles [11,12]. Electron diffraction and optical spectroscopy show that GaSe nanoparticles consist of single tetralayer structures (i.e., Se–Ga–Ga–Se sheets). Thus, they have a disklike, two-dimensional morphology and are exactly four atoms thick. This is an expected result, based on elementary chemical bonding considerations. There are strong covalent bonds within the Se–Ga–Ga–Se sheets, while only weak van der Waals forces hold adjacent sheets together. Detailed spectroscopic studies revealed that GaSe nanoparticles have highly anisotropic optical and quantum confinement prop-

* Corresponding author. Tel.: +86 0376 6393736.
E-mail address: syang@ucmerced.edu (S. Yang).

1010-6030/$ – see front matter © 2007 Elsevier B.V. All rights reserved.
doi:10.1016/j.jphotochem.2007.05.017

erties. InSe has the same crystal structure and similar lattice constants as GaSe, and would be expected to form similar disk-like nanoparticles. We also obtained many interesting results of InSe nanoparticles which have been published recently [13,14].

It is very important to understand the charge transfer mechanism between different materials. GaSe and InSe are ideal candidates for this purpose. On one hand GaSe and InSe have the same crystal structure and similar lattice parameters so it is convenient to grow epitaxially one onto the other. On the other hand, the energy band structures of these two materials permit charge transfer between them.

In this study, we present a synthetic method of GaSe/InSe core/shell nanoparticles, i.e., GaSe as core and InSe as shell, and the experiment results of the photophysicochemical properties of the GaSe/InSe core/shell nanoparticles. We also present some basic aspects of the relative energetic and charge transfer between GaSe core and InSe shell, based on their absorption spectra, static and time-resolved emission spectroscopy.

2. Experimental section

2.1. Materials

Trimethylgallium is purchased from strem chemicals and used without further purification. Methyllithium, trioctylphosphine (TOP) and trioctylphosphine oxide (TOPO) are purchased from Sigma–Aldrich. Anhydrous ether, tetrahydrofuran, selenium powder, and indium chloride are purchased from VWR. Trioctylphosphine and trioctylphosphine oxide are distilled under vacuum before use.

Trimethylindium/TOP solution is used in the synthesis of GaSe/InSe core/shell nanoparticles, and is prepared in the following way. $InCl_3$ (3.0 g, 13.56 mmol) is added in a flask and heated at 80 °C under vacuum for 1 h. The flask is cooled in an ice bath and purged with argon several times. Absolute ether (20 mL) is then injected and 25.4 mL of methyllithium ether solution (1.6 mol/L) is slowly added. Upon completion of this addition, the solution is stirred for 2 h. The trimethylindium is pumped off and collected in a liquid nitrogen cooled trap containing 13.5 mL of TOP. The trap is warmed to room temperature and the ether is then pumped off. The resulting 1 mol/L trimethylindium in TOP solution is stored in a dry box for further use. We find that the characteristics of this solution are identical with those of solutions made with commercial trimethylindium.

2.2. Measurements

The size distributions of GaSe and GaSe/InSe core shell nanoparticle samples are determined with transmission electron microscopy (TEM). This is done with a Jeol 2010 transmission electron microscope, operating at 200 kV. A small fraction of the nanoparticle solution is diluted with toluene by a factor of three, and a drop of the diluted solution is spread over a copper/Formvar grid (300 mesh size). The absorption spectra are measured on a HP 8452A spectrophotometer. The static emission spectra are obtained on a Spex Fluorolog-3 with a liquid nitrogen cooled CCD detector.

Time resolved emission results are obtained by time correlated single photon counting. In the apparatus used in these studies, the sample is excited with approximately 15 nJ, 2 ps pulses from the second harmonic of a Ti:sapphire laser (Spectra-Physics Millennia Vs/Tsunami) at a repetition rate of 82 MHz. The excitation wavelength is varied in the range of 400–450 nm with excitation spot sizes of about 3 mm. This combination of low pulse energies and relatively large spot sizes results in power densities that are sufficiently low that multiphoton excitations are expected to be completely avoided. Consistent with this expectation, we find that increasing or decreasing the power density by a factor of 10 has no effect on the observed kinetics.

Detection is accomplished with a Hamamatsu 6 mm MCP PMT and a time correlated single photon counting PC-board (SPC-630; Becker and Hickl GmbH). Wavelength selection is accomplished using a 0.25 m monochromator with a 150-groove/mm grating. The instrument response function is determined by observing the laser scatter, and is about 30 ps full width at half maximum. Polarized emission detection is accomplished using a Polaroid emission polarizer in a collinear or near collinear geometry. A polarization scrambler (Oriel) is used to eliminate the correction factors of the throughput of the monochromator.

SEM-EDAX is performed on a JSEM (Japan) coupled with a EDAX (Oxford), accelerating voltage is at 25 kV.

2.3. Synthesis of 6 nm GaSe nanoparticles

The GaSe nanoparticles are synthesized following a reported procedure [6]. A solution of 15 g of TOPO and 5 mL of TOP is heated to 150 °C overnight in nitrogen atmosphere. Commercial TOPO is typically wet, and this heating removes any water by reaction with TOP to form TOPO. Prior to making this solution, the TOP (technical grade from Aldrich) is vacuum distilled at 0.75 Torr, taking the fraction from 204 to 235 °C. A TOPSe solution made from 12.5 mL of TOP and 1.579 g Se (99.999%) is then added to the mixture. The above TOP/TOPO/TOPSe reaction mixture is heated to 278 °C. This is followed by the injection of 0.8 mL of GaMe [3] dissolved in 7.5 mL of distilled TOP. Upon injection, the temperature drops to 254 °C and 10 min later stabilizes at 266–268 °C. The presence of nanoparticles is indicated by the appearance of a 400–450 nm shoulder in the absorption spectrum. After this shoulder is formed, the reaction mixture is cooled to room temperature to prevent further reaction. Multiple injections of precursors are needed in order to grow monodispersed GaSe nanoparticles.

2.4. Synthesis of GaSe/InSe coreshell nanoparticles

Three millilitres above GaSe solution is added in a three-neck flask and heated to 256 °C. A total of 0.2 mL, 1 mol/L of $In(CH_3)_3$ solution and 0.2 mL, 1 mol/L of TOPSe solution are injected drop by drop, respectively, in 15 min. Upon injection the reaction mixture solution is cooled to 110 °C and stirred for 1 h, then cooled to room temperature.

3. Results and discussions

3.1. Synthesis and electron transitions

The synthetic method of GaSe nanoparticles has been reported [4–6]. One of the critical parameters in the synthesis of GaSe nanoparticles, regarding the average particle diameter and size distribution, is the reaction temperature. The optimal synthesis temperature is found to be 268 °C shortly after the injection of the $Ga(CH_3)_3$/TOP solution. Higher temperatures yield polydispersed nanoparticles, and at lower temperatures the reaction proceeds very slowly. The progress of the reaction and the nanoparticle size distribution are monitored by transferring a small aliquot of the reaction mixture to a cuvette and recording the absorption spectra. To obtain monodispersed nanoparticles, one sixth of the $Ga(CH_3)_3$ and TOPOSe precursors are added, respectively, at room temperature, then heated to 268 °C rapidly, kept at the temperature for 1 h and finally cooled to room temperature. This procedure can be repeated several times as needed.

GaSe and InSe are very similar in their crystallography and their crystal lattices match each other pretty well, so it is quite easy to form the core/shell structure with these two materials. In the synthesis of the GaSe/InSe core-shell nanoparticles, the $In(CH_3)_3$ is more reactive than $Ga(CH_3)_3$, so the InSe shell is formed at some lower temperature, 256 °C.

The densities of the bulk GaSe and InSe materials are taken as the basis of the calculation of the thickness of InSe shell. Calculations show that the thickness of the InSe shell is about 0.25 nm. Fig. 1 shows the TEM images of the GaSe and GaSe/InSe core/shell nanoparticles. The diameter of GaSe nanoparticles is measured to be about 6 nm in average. It is difficult to see this small difference between the GaSe and GaSe/InSe nanoparticles by their TEM images. A powder sample of the GaSe/InSe nanoparticles is prepared and its SEM-EDAX data are measured. The results are listed in Table 1. It can be seen that the molar ratio of Ga to In of the core/shell particles is 4.83, very close to that it should be, implying that core/shell particles formed.

The absorption spectra of the GaSe/InSe nanoparticles also show big difference. The absorption spectra of GaSe and GaSe/InSe nanoparticles are shown in Fig. 2. It is quite obvious about the difference of their absorption spectra. The onset of the red side just keep the same for these two samples, about 21,440 cm^{-1}, but the onset on the blue side shifts from 27,840 to 25,266 cm^{-1}, which means that the red side excitation mainly comes from the GaSe and InSe shell contributes little to the absorption of lower energy transition. The shift on the blue side absolutely results from the interaction between the GaSe core and the InSe shell.

Table 1
The SEM-EDAX data of GaSe/InSe core shell nanoparticles

Elements	wt.%	at.%	*Z*	*F*
Ga	35.40	33.79	1.0383	1.0058
Se	52.54	59.22	1.0023	1.0015
In	12.06	6.99	0.9794	1.0000

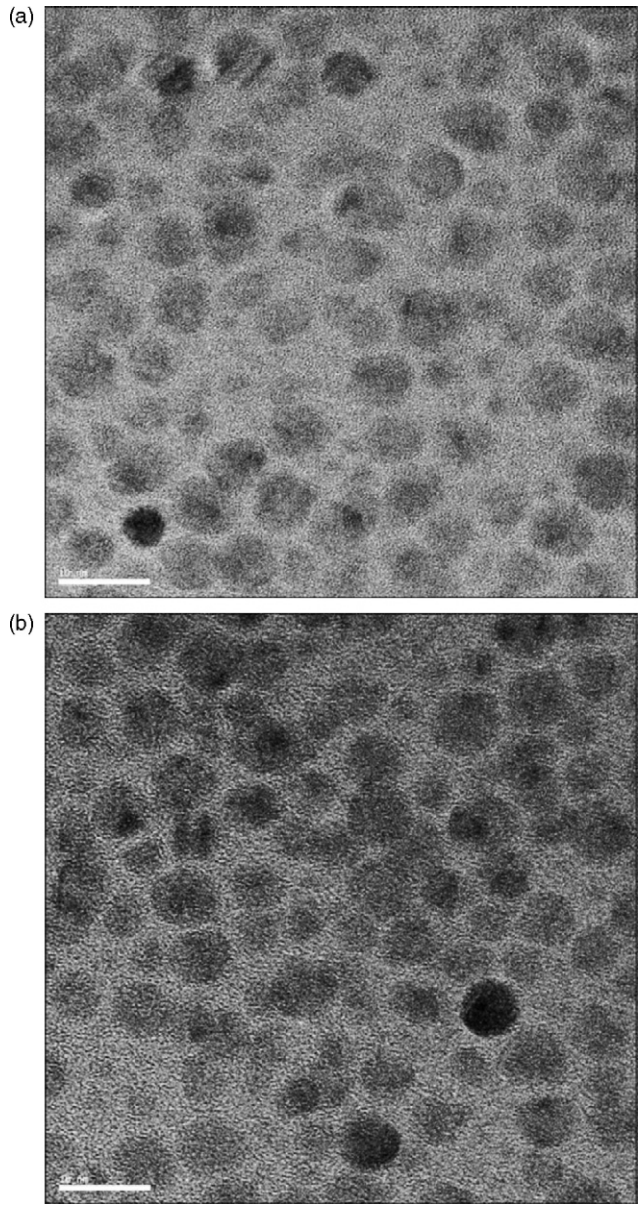

Fig. 1. (a) Transmission electron microscopy images of the GaSe nanoparticles. (b) Transmission electron microscopy images of the GaSe/InSe core/shell nanoparticles.

The energy band structure consideration will facilitate the interpretation of the spectroscopic properties of the GaSe and GaSe/InSe core/shell nanoparticles. Bulk GaSe is an indirect band gap semiconductor with a band gap of about 2.11 eV (588 nm) [15,16]. The absorption onsets in Fig. 1 are shifted into the 400–460 nm region. This absorption onset is shifted 5000–8000 cm^{-1} to the blue of the bulk GaSe absorption onset (588 nm), in accord with quantum confinement theories of semiconductor nanoparticles. In the band structure of GaSe the top of the valence band is at Γ and the bottom of the conduction band is at M. The direct and indirect absorption transitions correspond to a Γ_4^- to Γ_3^+ and Γ_4^- to M_3^+ transitions, respectively. The direct band gap is at a very slightly higher energy, about 25 meV above the indirect band gap. The direct transition corresponds to a Γ_4^- to Γ_3^- transition, and is polarized along the *z* axis, perpendicular

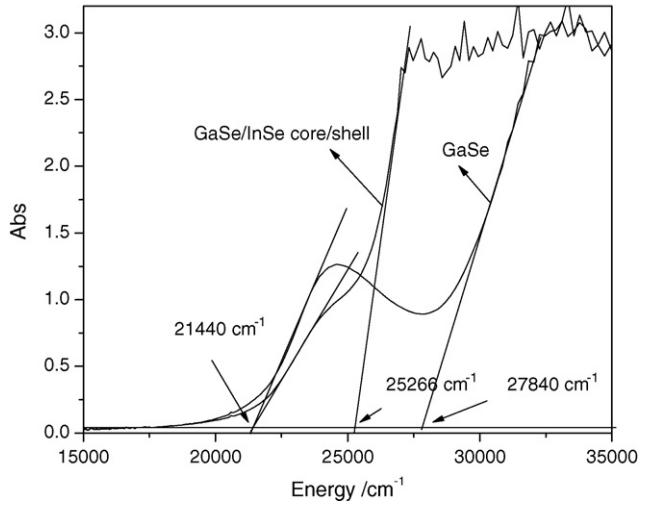

Fig. 2. Plots of absorbance vs. energy for the GaSe nanoparticles and GaSe/InSe core/shell nanoparticles. Also shown are the extrapolations to zero used to determine approximate band gaps in each case.

to the basal planes. Γ_3^- is not energetically close to any other electronic state at Γ and conduction band mixing can be ignored. On the other hand, there are four valence band states (Γ_5^+, Γ_5^-, Γ_6^+ and Γ_6^-) in proximity to Γ_4^-, with which mixing can occur, and the Γ_4^- band mixes through spin–orbit coupling with the Γ_6^- band. As a result, the Γ_6^- to Γ_3^+ transition is allowed and is *x–y* polarized. Thus, the Γ_4^-/Γ_6^- mixing results in an *x–y* polarized component in the direct band edge transition. Since the hole state is the same for both the direct and indirect transitions, the indirect transition has the same polarization properties as the direct transition.

Bulk InSe has a room temperature absorption onset at 1.24 eV (1000 nm)[2] [2]. In the case of bulk InSe, the top of the valence band and the bottom of the conduction band are both at Γ and the lowest energy transition is therefore momentum allowed; it is a "direct" transition [2,3]. A slightly higher (750 cm^{-1}) local minimum of the conduction band is at the M point and the corresponding Γ−M transition is a much less intense, momentum forbidden "indirect" transition [17].

Fig. 3 shows the energetic diagrams of GaSe and InSe, and also shown are the electron transitions [7,13].

In many conventional core/shell nanoparticles, charge transfer can be observed. Red edge shift to longer wavelengths accompanying shell growth was observed [18,19], but there is some case that the red edge did not change and a blue shift is even expected [20]. In our case GaSe and InSe are single four atom layer disk-like nanoparticles, so the InSe shell is only formed on the peripheries of GaSe cores while the surface (0 0 1) is still free. The absorption onset of the GaSe cores is nearly maintained, indicating that the size is well preserved. The GaSe cores were excited directly. Transitions in the GaSe cores (21,440 cm^{-1} from the Γ_4^- to Γ_3^+ and 27,840 cm^{-1} from the Γ_6^- to Γ_3^+ of the GaSe cores) and from the GaSe cores to the InSe shell (25,266 cm^{-1} from the Γ_4^- of GaSe core to the Γ_3^+ of InSe shell) are observed in these GaSe/InSe nanoparticles.

3.2. Steady-state emission spectra and transition

The emission spectra of the GaSe and the GaSe/InSe core shell nanoparticles obtained following excitation between 360 and 460 nm are shown in Fig. 4. The excitation wavelength dependence is mostly associated with the different sizes of GaSe and GaSe/InSe core/shell nanoparticles. Excitation on the red edge of the absorption onset excites only the largest particles, while further blue excitation is not size selective. As a result, the emission following red-edge excitation is narrower and shifted further to the red. The emission is the most intense following

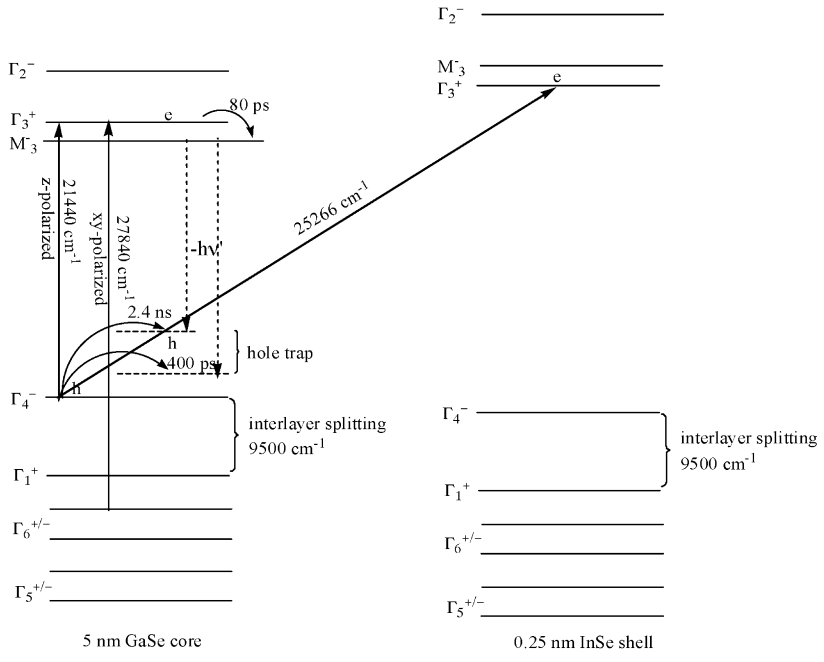

Fig. 3. Energy band structures of the GaSe core and InSe shell. Also shown is the charge transfer between them.

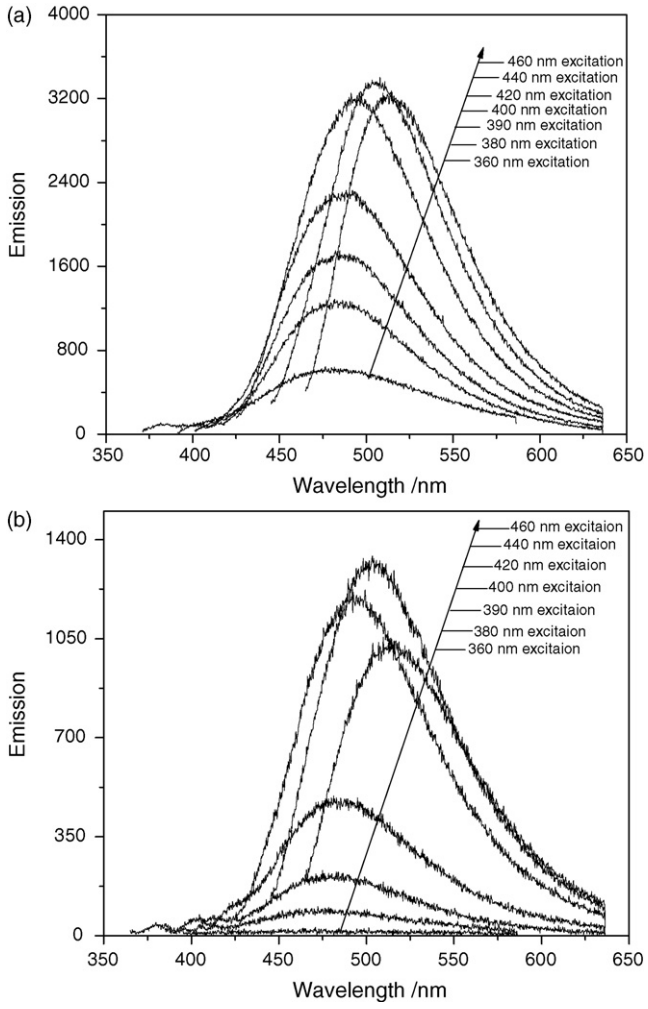

Fig. 4. (a) Steady-state emission spectra correlation with excitation of the GaSe nanoparticles and GaSe/InSe core/shell nanoparticles. (b) Steady-state emission spectra correlation with excitation of the GaSe/InSe core/shell nanoparticles.

excitation at 430 nm, which is the peak of the GaSe nanoparticle optical density.

Compared with the GaSe nanoparticles, the emission intensity of the GaSe/InSe nanoparticles decreased drastically but the positions of the emission peaks just stay the same, which means that the emission mainly comes from the GaSe cores while the InSe shell did not emit. On one hand, the trap states of GaSe cores can be suppressed as an InSe shell is grown on the surface of the GaSe core, which results in enhanced emission. On the other hand, the electron transition from the GaSe core to the InSe shell (25,266 cm^{-1} from the Γ_4^- of GaSe core to the Γ_3^+ of InSe shell) follows a non-radiation relaxation, which results in decreased emission of the GaSe core. The fact that emission was quenched in the GaSe/InSe nanoparticles demonstrates that the latter plays a greater role in the relaxation.

Assignment of the transitions observed in the absorption spectra and depicted in Fig. 3 is also facilitated by emission polarization measurements. As shown earlier the GaSe and GaSe/InSe coreshell nanoparticles are disklike nanoparticles and have an anisotropic nature. Their emission is polarized and the polarization can give much information about the assignment of the excited states. The emission polarization is characterized by the anisotropy, r, given by [21]

$$r = \frac{I_{par} - I_{perp}}{I_{par} + 2I_{perp}} = \frac{1}{5}(3\ \cos^2\theta - 1) \quad (1)$$

where I_{par} and I_{perp} are the emission intensities polarized parallel and perpendicular to the polarization of the excitation light, respectively, and θ is the angle between the emission and excitation transition oscillators. Several limiting cases are of interest. The case of collinear excitation and emission oscillators results in the largest possible anisotropy for an incoherent process, 0.40. Similarly, the case of coplanar excitation and emission oscillators requires integration over the plane and gives an anisotropy of 0.10. If the excitation and emission oscillators are at 90° angles, an anisotropy of −0.20 is obtained.

Fig. 5 shows the emission anisotropy of the GaSe and GaSe/InSe coreshell nanoparticles excited at 420 nm. This anisotropy has a value of about 0.15. This is >0.10, the value associated with coplanar absorption and emission oscillators,

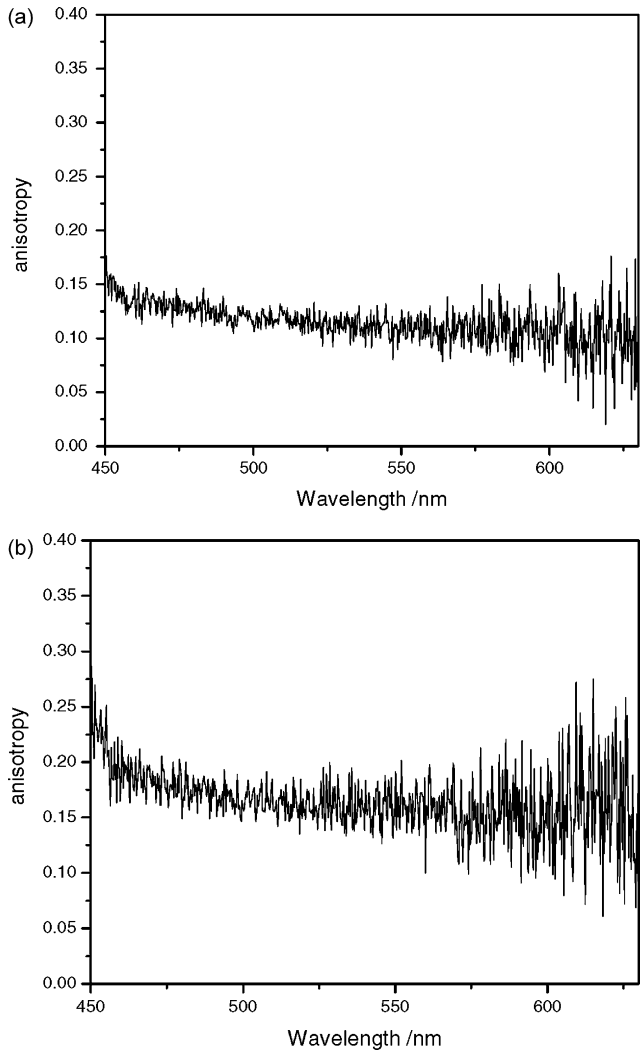

Fig. 5. (a) Emission anisotropy of the GaSe nanoparticles. (b) Emission anisotropy of the GaSe/InSe core/shell nanoparticles. Both samples are excited with 420 nm light.

and we conclude that this emission can only result from the excitation and emission oscillators being collinear or nearly linear oscillators. With the disklike geometry of these nanoparticles, this transition is only assigned to excitation and emission occurring along the z axis, perpendicular to the plane of the nanoparticles. Consistent with the polarization results in bulk InSe [3], the low-energy absorption can be assigned to excitation of the band edge state. Emission occurs from this state and/or other states that derive oscillator strength from it. The GaSe and the GaSe/InSe nanoparticles almost have the same anisotropy as shown in Fig. 5, which means that the disk geometry of The GaSe core does not change as the forming of the InSe shell and the electrons in the conduction band of InSe relax in a nonradiative way.

3.3. Time resolved emission spectra and relaxation dynamics

Relaxation dynamics can give more information about the transition and relaxation processes in the GaSe and GaSe/InSe coreshell nanoparticles. The emission decay curves following 420 nm excitation are shown in Fig. 6. The detection wavelength is 485 nm, the maximum of the static emission spectrum.

To understand the dynamical results presented here, it is first necessary to analyze some of the crystal structure and energetic differences and similarities between GaSe and the GaSe/InSe core/shell nanoparticles. Nanoparticles generally have very high surface to volume ratios, and are thus expected to have large numbers of trap states. We may therefore, expect electron traps and hole traps in the GaSe nanoparticles. When an InSe shell is formed on the surface of a GaSe nanoparticle, some surface defects of the GaSe nanoparticle are effectively suppressed; as a result there will be fewer traps in the GaSe/InSe core/shell nanoparticles. The differences in their emission kinetics can be addressed by their different trap states. The relaxation processes responsible for the observed spectroscopic transients are summarized and discussed below.

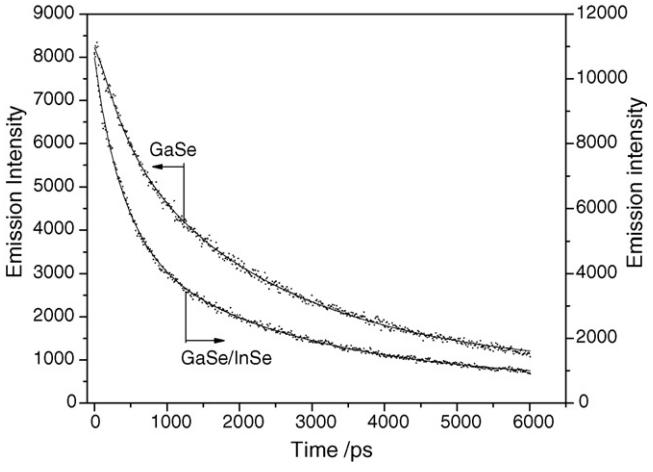

Fig. 6. Emission decay curves of the GaSe nanoparticles and GaSe/InSe core/shell nanoparticles. Excited at 420 nm and detected at 485 nm. Also shown are curves fitted to the emission decay having 80 ps, 400 ps and 2.4 ns components.

The decay curves in Fig. 6 can be best fit by the sum of three exponentials, having time constants of 80 ps, 400 ps and 2.4 ns. In our earlier report it is shown that the 80 ps is the electron of the conduction band relaxation time while the 400 ps is the shallow hole trap relaxation time and 2.4 ns the deep hole trap relaxation time [7].

Although, the 400 ps and 2.4 ns time constants exist in both GaSe and GaSe/InSe core/shell nanoparticles, the amplitudes are very different. In the case of GaSe nanoparticles the 400 ps component accounts for 29% and the 2.4 ns component accounts for 71%, while in GaSe/InSe core/shell nanoparticles the 400 ps component accounts for 54% and the 2.4 ns component accounts for 46%. The results demonstrate that there are fewer deep hole traps in the GaSe/InSe coreshell nanoparticles than the GaSe nanoparticles. The InSe shells suppress the deep hole traps of the GaSe cores.

Again, the polarization kinetics can give further evidence of the suppression of the deep hole traps in the GaSe/InSe core/shell nanoparticles. As shown in Fig. 3, in GaSe electron transitions involving trapped electrons can gain oscillator strength by mixing of the electron trap level (M_3^+) with the only nearby conduction band level, Γ_3^+. Thus, these transitions will have the same polarization characteristics as those involving electrons in the Γ_3^+ state. The situation is more complicated for trapped holes. Hole trap states can mix with all of the nearby valence band levels (Γ_4^-, Γ_5^+, Γ_5^-, Γ_6^+ and Γ_6^-). The relative extents of this mixing will depend on the energy separations. Very shallow hole traps are expected to mix primarily with the highest valence band level, Γ_4^-. Transitions involving these holes are, therefore, expected to have polarization characteristics similar to those of the direct excitation. As the hole trap gets deeper, mixing with all of the nearby valence band levels will occur more or less equally. Only the Γ_4^- and Γ_6^- levels have allowed transitions to the conduction band Γ_3^+ level. Since the transitions involving the Γ_4^- and Γ_6^- levels give rise to z and x–y polarized emission, respectively, emission from hole trap levels that mix with both of these bands is expected to be unpolarized. The important conclusion is that hole trapping, but not electron trapping, results in loss of emission polarization, and that the deeper the hole trap, the more the emission is depolarized [7].

Fig. 7 shows the decay curves of the anisotropy of GaSe and GaSe/InSe core/shell nanoparticles excited at 420 nm and detected at 485 nm. The initial anisotropy value of about 0.325 indicates that most of the emission comes from the absorption oscillator or from an oscillator aligned with the absorption oscillator. Since the z axis is unique, most of the emission must be polarized along this axis. The observed initial anisotropy 0.325 is, however, somewhat below the linear oscillator value of 0.40, indicating that some of the emission is from an in-plane oscillator ($\theta = 90$ in Eq. (1)).

The anisotropy undergoes biphasic decay with 400 ps and 2.4 ns components. These decay components match the longer decay components in the emission kinetics, Fig. 6. The early time anisotropy decay is best fit by the 400 ps component. Thus, the process which results in the 80 ps decay of the total emission intensity causes no change in the emission anisotropy. Since the extent of the emission polarization is controlled by the mixing

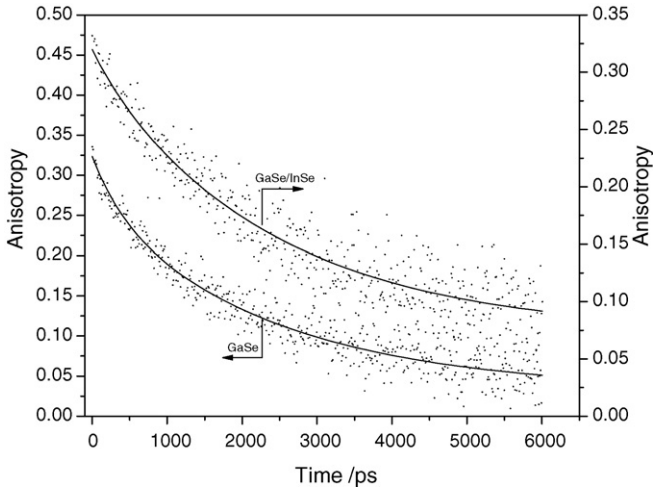

Fig. 7. Emission anisotropy decay curves of the GaSe nanoparticles and GaSe/InSe core/shell nanoparticles. Excited at 420 nm and detected at 485 nm. Also shown are curves fitted to the anisotropy decay having 400 ps and 2.4 ns components.

of the valence band states, the observation that the anisotropy also has a decay component with this time constant indicates that this transient is associated with hole relaxation. The most reasonable assignment for this transient is that it corresponds to hole localization in shallow traps. Similarly, the 2.4 ns component corresponds to hole localization in deep traps.

Once again, although the 400 ps and 2.4 ns time constants exist in both GaSe and GaSe/InSe core/shell nanoparticles, the amplitudes are very different. In GaSe nanoparticles the 400 ps component accounts for 21% and the 2.4 ns component accounts for 79%, while in GaSe/InSe core/shell nanoparticles the 400 ps component accounts for 6% and the 2.4 ns component accounts for 94%. It should be kept in mind that it is hole trapping that results in loss of emission polarization, and that the deeper the hole trap, the more the emission is depolarized. So the conclusion is that the more the deep hole traps, the faster does the decay of anisotropy. There is more 2.4 ns component in the GaSe/InSe core/shell nanoparticles, so its anisotropy decreases more slowly, which means that there are fewer deep hole traps in these nanoparticles.

4. Conclusion

GaSe/InSe core/shell nanoparticles are synthesized by a high temperature pyrogenation of organometallic precursors. The results presented here show that following photoexcitation, the GaSe/InSe core/shell nanoparticles emit intense, polarized emission. A charge transfer process accounts for the absorption and emission differences between GaSe and GaSe/InSe core/shell nanoparticles. Several dynamical relaxation processes depolarize and attenuate the intensity of this emission. Emission decay takes place on the 80 ps, 400 ps, and 2.4 ns time scales, while anisotropy decay follows two stages of 400 ps and 2.4 ns. Relaxation kinetics shows that the deep hole traps are effectively suppressed in the GaSe/InSe core/shell nanoparticles. As a result, the emission of the GaSe/InSe core/shell nanoparticles decays faster but the anisotropy decays slower than the GaSe nanoparticles.

Acknowledgment

The authors thank a grant from the Department of Energy (Grant No. DE-FG03-00ER15037) and the start-up foundation of Xinyang Normal University for the financial support of this work.

References

[1] F. Levy, Crystallography and Crystal Chemistry of Materials with Layered Structures, Reidel, Dordrecht, The Netherlands, 1976, 32–35.
[2] J. Camassel, P. Merle, H. Mathieu, A. Chevy, Excitonic absorption edge of indium selenide, Phys. Rev. B 17 (1978) 4718–4725.
[3] V.P. Savchyn, V.B. Kytsai, Photoelectric properties of heterostructures based on thermooxidated GaSe and InSe crystals, Thin Solid Films 361–362 (2000) 123–125.
[4] J. Martinez-Pastor, A. Segura, C. Julien, A. Chevy, Shallow-donor impurities in indium selenide investigated by means of far-infrared spectroscopy, Phys. Rev. B 46 (1992) 4607–4616.
[5] O. Lang, A. Klein, C. Pettenkofer, W. Jaegermann, A. Chevy, Band lineup of lattice mismatched InSe/GaSe quantum well structures prepared by van der Waals epitaxy: absence of interfacial dipoles, J. Appl. Phys. 80 (1996) 3817–3821.
[6] V. Chikan, D.F. Kelley, Carrier relaxation dynamics in GaSe nanoparticles, Nano Lett. 2 (2002) 1015–1020.
[7] V. Chikan, D.F. Kelley, Relaxation dynamics in photoexcited GaSe nanoparticles, J. Chem. Phys. 117 (2002) 8944–8952.
[8] V. Chikan, D.F. Kelley, Synthesis of highly luminescent GaSe nanoparticles, Nano Lett. 2 (2002) 141–145.
[9] V. Chikan, D.F. Kelley, Size-dependent spectroscopy of MoS_2 nanoclusters, J. Phys. Chem. B 106 (2002) 3794–3804.
[10] H.H. Tu, V. Chikan, D.F. Kelley, Electron and hole intraband spectroscopy of GaSe nanoparticles, J. Phys. Chem. B 107 (2003) 10389–10397.
[11] H.H. Tu, S.M. Yang, V. Chikan, D.F. Kelley, Spectroscopy of GaSe nanoparticle aggregates, J. Phys. Chem. B 108 (2004) 4701–4710.
[12] H.H. Tu, K. Mogyorosi, D.F. Kelley, Exciton dynamics of GaSe nanoparticle aggregates, J. Chem. Phys. 122 (2005) 44709–44722.
[13] S.M. Yang, D.F. Kelley, The spectroscopy of InSe nanoparticles, J. Phys. Chem. B 109 (2005) 12701–12709.
[14] S.M. Yang, D.F. Kelley, Transient absorption spectra and dynamics of InSe nanoparticles, J. Phys. Chem. B 110 (2006) 13430–13435.
[15] V. Grasso, Electronic Structure and Electronic Transitions in Layered Materials, Reidel, Dordrecht, 1986, 108–110.
[16] M.O.D. Camara, A. Mauger, I. Devos, Electronic structure of the layer compounds GaSe and InSe in a tight-binding approach, Phys. Rev. B 65 (2002) 125206–125212.
[17] F.J. Manjon, D. Errandonea, A. Segura, V. Munoz, G. Tobıas, E. Canadell, Experimental and theoretical study of band structure of In Se and $In_{1-x}Ga_xSe$ under high pressure: indirect crossovers, Phys. Rev. B 63 (2001) 125330–125343.
[18] B.O. Dabbousi, J. Rodriguez-Viejo, F.V. Mikulec, J.R. Heine, H. Mattoussi, R. Ober, K.F. Jensen, M.G. Bawendi, (CdSe) ZnS core-shell quantum dots: synthesis and characterization of a size series of highly luminescent nanocrystallites, J. Phys. Chem. B 101 (1997) 9463–9475.
[19] Y.W. Cao, U. Banin, Synthesis and characterization of InAs/InP and InAs/CdSe core/shell nanocrystals, Angew. Chem. Int. Ed. 38 (No. 24.) (1999).
[20] X.G. Peng, M.C. Schlamp, A.V. Kadavanich, A.P. Alivisatos, Epitaxial growth of highly luminescent CdSe/CdS core/shell nanocrystals with photostability and electronic accessibility, J. Am. Chem. Soc. 119 (1997) 7019–7029.
[21] A. Albrecht, Polarizations and assignments of transitions: the method of photoselection, J. Mol. Spectrosc. 6 (1961) 84–108.